Geothermics 57 (2015) 196–204

Contents lists available at ScienceDirect

Geothermics

journal homepage: www.elsevier.com/locate/geothermics

Prediction of reinjection effects in fault-related subsidiary structures by using fractional derivative-based mathematical models for sustainable design of geothermal reservoirs

Anna Suzuki [a,*], Yuichi Niibori [b], Sergei Fomin [c], Vladimir Chugunov [d], Toshiyuki Hashida [e]

[a] Stanford University, 367 Panama Street, Green Earth Science Bldg. 080C, Stanford, CA 94305-2220, USA
[b] Tohoku University, 6-6-01-2, Aramaki-Aza-Aoba, Aoba, Sendai 980-8579, Japan
[c] California State University, Chico, CA 95929, USA
[d] Kazan Federal University, Kazan 420008, Russia
[e] Tohoku University, 6-6-11-709, Aramaki-Aza-Aoba, Aoba, Sendai 980-8579, Japan

ARTICLE INFO

Article history:
Received 3 September 2014
Received in revised form 3 April 2015
Accepted 10 April 2015
Available online 18 July 2015

Keywords:
Reinjection
Fault zone
Fractal
Tracer test
Fractional advection-dispersion equation (fADE)

ABSTRACT

This study provides a method to evaluate the effects of cold-water injection into an advection-dominated geothermal reservoir. A fractional advection-dispersion equation (fADE) and a fractional heat transfer equation (fHTE) are applied to fault-related structures in geothermal areas where the fracture density is described by a power-law model. Synthetic production data generated by a numerical reservoir simulator reveal that the fADE and the fHTE are in reasonable agreement with the tracer responses and temperature change in a fault zone. Tracer analysis based on the fADE has potential to elucidate fault-related structures and to predict premature thermal breakthroughs quickly and efficiently.

1. Introduction

Geothermal energy is a promising energy source for stable generation of electricity regardless of the weather or time of day. Most geothermal power plants extend the lifespan of the resources by sustaining the amount of water and pressure within the reservoir. Reinjection is of great importance for sustainable utilization of geothermal systems, which has been discussed in Axelsson (2010) and Kaya et al. (2011). One of the major problems with this reinjection process, however, is the possibility of an early thermal breakthrough in production areas. There remains a need to establish criteria and guidelines for sustainable reinjection operations that allow us to design the location of wells, injection temperatures, and/or flow rates.

Fracture and fracture networks contribute critically to fluid flow and heat propagation. In a geothermal reservoir, structures associated with large-scale faults appear to be quite important in controlling fluid flow (Massart et al., 2010). The simplest description of a fault zone structure (and fault zones in general) considers two major mechanical units, namely a fault core and a damage zone (cf., Caine et al., 1996; Faulkner et al., 2010). The fault core is formed through repeated slipping of the principal fault plane and is composed of impermeable barriers. The damage zone consists of a volume of deformed rocks with smaller fractures around a fault surface that results from slips along faults (Caine et al., 1996). In the fault damage zone, the fracture density (the number of fractures per unit length) commonly increases near the fault core (e.g., Brock and Engelder, 1977; Chester and Logan, 1986; Agosta and Kirschner, 2003; De Joussineau and Aydin, 2007; Gudmundsson, 2011). Savage and Brodsky (2011) found that isolated single faults with small displacements have macrofracture densities that decay as a power law. The power-law function is a feature of fractal geometry, which provides widely applicable and descriptive tools for characterization of subsurface fracture systems (Bonnet et al., 2001).

Tracer testing is a standard method for evaluating fluid flow within a geothermal reservoir. Tracer responses often observed in geothermal fields include non-Gaussian leading or trailing edges (also called heavy tails) of a plume emanating from a point source, or nonlinear growth of the centered second moment (e.g., Sanjuan et al., 2006). Numerous numerical experiments indicate that anomalous dispersion cannot be described by the traditional second-order advection-dispersion equation (ADE) that is based

* Corresponding author. Tel.: +1 6507395018.
E-mail address: anna3@stanford.edu (A. Suzuki).

http://dx.doi.org/10.1016/j.geothermics.2015.04.001
0375-6505/

Nomenclature

a	arbitrary constant
b	retardation coefficient for tracer
c	tracer concentration
C	non-dimensional concentration of tracer
Cp	heat capacity
d	arbitrary constant
D	dispersion coefficient
dx	grid spacing
dy	grid spacing
e	retardation parameter for heat
fADE	fractional advection-dispersion equation
FD	fracture density
fHTE	fractional heat transfer equation
FW	foot wall
H	thickness of calculation domain
HW	hanging wall
K	permeability
l	representative length
L	length of the calculation domain
n	exponent describing decay of fracture density
p	Skewness parameter
Pe	Péclet number
R^2	coefficient of determination
RMSE	root mean square error
t	time
t_{tracer}	characteristic time of tracer migration
T	non-dimensional temperature
v	Darcy velocity
x	horizontal coordinate
X	non-dimensional distance
y	horizontal coordinate
α	order of spatial fractional derivative in fADE
β	order of temporal fractional derivative in fADE
β'	order of temporal fractional derivative in fHTE
γ	order of temporal fractional derivative in fADE
γ'	order of temporal fractional derivative in fHTE
θ	exponent describing decay of permeability
Θ	temperature
ξ	exponent describing decay of diffusivity
μ	viscosity
ρ	density
τ	non-dimensional time
ϕ	porosity

Subscripts

0	reference value
1	surrounding rock
2	main conduit
3	matrix
i	node index
in	injection
o	initial
r	rock
w	water

on Fick's diffusion law (Adams and Gelhar, 1992). To describe such tracer behaviors, several alternative mass transport models have been developed. Fractional differential equations have been demonstrated to simulate the anomalous characteristics of solute transport in highly heterogeneous media (Benson et al., 2000; Baeumer et al., 2001; Schumer et al., 2003). Using fractional derivatives in time and space, Fomin et al. (2005, 2011) derived the fractional advection-dispersion equation (fADE). The fADE accounts for the diffusion of solute into surrounding rocks based on a fractal diffusion coefficient. In the last decade, many authors have made notable contributions to both the theory and the application of fADE in hydrology, as reviewed by Zhang et al. (2009).

The transport properties of tracers cause the chemical front to be close to the thermal front. Because the chemical front of the tracers arrives earlier than the heat front does, the tracer response can be used as an indicator of thermal breakthrough. Migration of the cold-water front for a single-phase flow is fairly well understood from the work of Lauwerier (1955) and Bodvarsson (1972). Subsequently, other work has estimated temperature changes over time at the production wells (Gringarten and Sauty, 1975; Bödvarsson and Tsang, 1982; Shook, 2001; Kocabas, 2005). When advection is dominant, the retardation of the thermal front in comparison to the hydrodynamic front can be described by the ratio of rock/water volumetric heat capacities. This assumption has been widely used to estimate cooling effects of reinjected fluid in several geothermal fields but leads to overestimation of the temperature decline (e.g., Aksoy et al., 2008). There is a possibility of heat conduction into the surrounding rocks, which may play an important role in the temperature change in fractured reservoirs. In these models, the tracer is assumed to migrate along preferential flow paths (fractures), and the breakthrough time is essentially a measure of the total volume of the path between injection and production wells. Thermal migration, on the other hand, is determined by the surface area for thermal conduction from the reservoir rocks to the preferential flow path (Pruess and Bodvarsson, 1984; Shook, 2003).

López and Smith (1995) examined the interaction between thermally driven circulation in a fault zone and the surrounding rocks. They mapped fluid flow and heat transfer regimes in different permeability regions of the fault and the surrounding rocks. For fault permeabilities lower than 7×10^{-13} m^2 and rock permeabilities lower than 5×10^{-18} m^2, conduction was the dominant transport mechanism, while advection dominated for rock permeabilities higher than 5×10^{-18} m^2. In the former case, the effect of thermal conductivity of the surrounding rocks cannot be ignored. In the latter case, the surrounding rocks are relatively permeable, which may be due to small fractures around the fault in damage zones. In this case, the thermal migration can be advective, which causes a lag behind the fluid front by a constant related to the ratio of rock/water volumetric heat capacities. Our previous study (Suzuki et al., 2014) proposed the fractional heat transfer equation (fHTE) based on the fADE to characterize diffusion into surrounding rocks by using fractional derivatives in the same manner as the fADE. The fHTE considers that thermal diffusion occurs as a result of hydrodynamic mixing of the fluid particles passing through the surrounding rocks. This heat transfer due to fluid flow is of importance when advection is dominant.

Little has been reported on quantitative investigations of fracture density and spatial distributions at a damage zone in a geothermal field. First, using data from the literature, we demonstrated that the fracture distributions in a geothermal reservoir are accurately characterized by power-law functions. Then, the relationship between the fault-related structure and the fADE and the fHTE were explained. A numerical reservoir simulator, TOUGH2, was used to generate production data in an advection-dominated reservoir to verify the applicability of the fADE and the fHTE. Finally, we proposed a method of analyzing tracer responses for characterizing fault-related structures.

2. Mathematical model

Field observations in geothermal reservoirs indicate that main permeable zones are typically formed by fault-related structures,

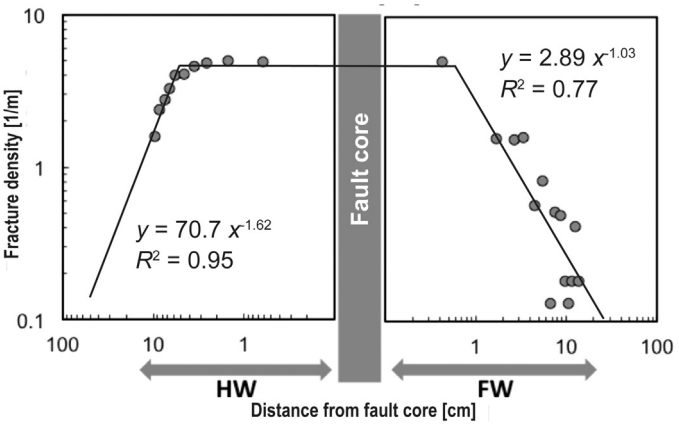

Fig. 1. Fracture density in the Rapolano geothermal area (after Brogi, 2008).

which can include fault cores and damage zones (Caine et al., 1996). Savage and Brodsky (2011) suggested that fracture density, *FD*, at a damage zone decays with distance from the fault core according to the following power law:

$$FD(y) = FD_0 y^{-n}, \tag{1}$$

where FD_0 is the constant of fracture density, y is the distance from the fault core, and n is the exponent describing the decay of fracture density.

We evaluated whether the power-law model of fracture density is applicable to fault zone architectures in a geothermal reservoir. Brogi (2008) investigated the structural architectures of 13 normal faults in the Rapolano geothermal area (hinterland of the Northern Apennines, Italy). The frequency distribution for the fracture density is shown in Fig. 1. The hanging wall (HW) is the block positioned over the fault core, and the foot wall (FW) is positioned under it. Fig. 1 indicates that fractures are developed in both the foot wall and hanging wall. The best-fit power-law approximations are also plotted. Nearly constant fracture density can be observed around the fault core. This high fracture density area may control fluid flow in the reservoir and provide main conduits. In contrast, the surrounding area shows decreases in fracture density with the distance in accordance with the power law approximations.

The fracture distribution plotted in Fig. 1 was observed at the outcrop scale. Le Garzic et al. (2011) presented a multi-scale mapping of fracture systems and indicated that the fracture network is described by a fractal behavior in tectonic systems. Because of the self-similarity in the structure and the pattern of the fractures, the fracture distribution at the reservoir scale also may exhibit similar trends. Hence, the power-law approximation of the fracture density can characterize the fracture distribution at the field scale in a geothermal reservoir.

Fomin et al. (2011) proposed the fractional advection-dispersion equation (fADE) to model solute transport in a fracture system. Detailed descriptions of the mass transport model can be found in the literature (Fomin et al., 2005, 2011). The schematic of a fractured reservoir for the fADE is represented in Fig. 2. At a field scale, a fault zone system consists of a fault core and damage zones. The damage zone forms a main conduit along the fault core. At this scale, the major flow is assumed to be one dimensional in the x-axis direction. Diffusion into the surrounding rocks also occurs in the y-axis direction. When the main conduit is downscaled, one can find complex fracture networks. Furthermore, at a smaller scale, the rock matrix includes secondary branched fractures. The governing equation of mass transport was developed in the following form (Fomin et al., 2011):

$$\frac{\partial \phi_2 c_2}{\partial t} + a_3 \frac{\partial^\gamma c_2}{\partial t^\gamma} + a_1 \frac{\partial^\beta c_2}{\partial t^\beta} = D_2 \frac{\partial}{\partial x}\left(p \frac{\partial^\alpha c_2}{\partial x^\alpha} + (1-p) \frac{\partial^\alpha c_2}{\partial (-x)^\alpha} \right) - v \frac{\partial c_2}{\partial x}, \tag{2}$$

where t is time and x is the distance from an injection zone. Variables c_2 and ϕ_2 are the concentration of tracer and the porosity in the main conduit, respectively. Parameters D_2 and v are the dispersion coefficient and the Darcy velocity in the main conduit. Note that the subscripts 1, 2, and 3 were used to designate the variables in the surrounding rocks, the main conduit, and the matrix. Parameters a_1 and a_3 are the retardation coefficient related to diffusion processes in the surrounding rocks and in the matrix. The skewness parameter is given by p (Huang et al., 2008). Parameters $\alpha (0 < \alpha \leq 1)$, $\beta (0 < \beta \leq 1)$and $\gamma (0 < \gamma \leq 1)$ are the orders of the fractional derivatives.

The fADE is capable of describing diffusion into the surrounding rocks by using the third term in Eq. (2) based on a diffusion equation formulated according to fractal geometry (Samko et al., 1993). The diffusion equation includes a fractal diffusion coefficient given by:

$$D(y) = D_0 y^{-\xi}, \tag{3}$$

where D_0 is the constant, y is the distance perpendicular to the direction of main flow, and ξ is the exponent describing the decay of diffusivity. When fracture density decreases with distance as described in Eq. (1), it is likely that the diffusion coefficient also changes spatially. In this study, we assume that the fractal diffusion coefficient given by Eq. (3) describes the diffusion processes from the main conduit into the surrounding rocks in a damage zone.

In order to normalize Eq. (2), non-dimensional variables and modified retardation coefficients are introduced as follows:

$$\tau = \frac{t}{t_{tracer}}, \quad X = \frac{x}{l}, \quad C = \frac{c_2}{c_{in}}, \quad Pe = \frac{v l^\alpha}{D_2}, \quad b_1 = \frac{a_1}{\phi_2} t_{tracer}^{1-\beta}, \quad b_3 = \frac{a_3}{\phi_2} t_{tracer}^{1-\gamma}; \tag{4}$$

where t_{tracer}, l, and c_{in} are the representative values of time, length, and concentration, respectively. We set the representative length, l, to the distance between the inlet and the outlet. The representative time, t_{tracer}, is the period during which tracer migrates the distance, l, at the velocity, v. The representative concentration, c_{in}, was the injected concentration of tracers. Pe was the Péclet number.

By using the above non-dimensional variables, the normalized governing equation of Eq. (2) can be written as:

$$\frac{\partial C}{\partial \tau} + b_3 \frac{\partial^\gamma C}{\partial \tau^\gamma} + b_1 \frac{\partial^\beta C}{\partial \tau^\beta} = \frac{1}{Pe} \frac{\partial}{\partial X}\left(p \frac{\partial^\alpha C}{\partial X^\alpha} + (1-p) \frac{\partial^\alpha C}{\partial (-X)^\alpha} \right) - \frac{\partial C}{\partial X}. \tag{5}$$

Here, the first term on the left side is an accumulation term, and the second term models a retardation process associated with diffusion into matrices induced by the secondary branched fractures. The third term describes a process of diffusion into the surrounding rocks. The first term on the right side expresses dispersion within the main conduit, and the second term is an advection term. When the values of b_1 and b_3 are set to 0 and the order of spatial fractional derivative α is set to 1, Eq. (5) is consistent with the conventional advection-dispersion equation (ADE) (Bear, 1972).

The analogous behaviors of heat and mass transfer have long been recognized (Welty et al., 2009). Because of this analogy, the fractal geometry may lead to characterization of the thermal diffusion in the same manner as solute diffusion. The governing

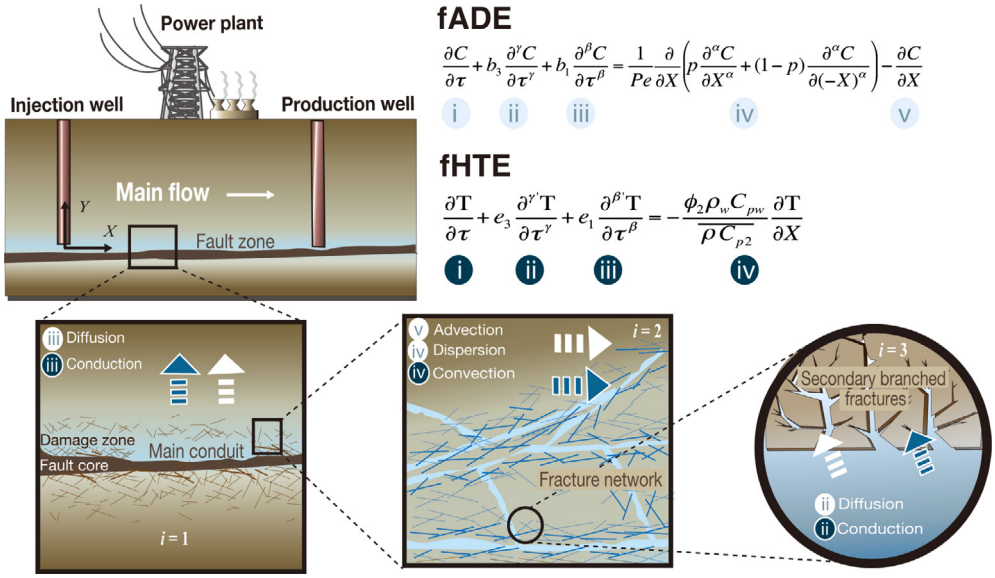

Fig. 2. Schematic of a fractured reservoir.

equation to model heat transfer, which is called the fractional heat transfer equation (fHTE), has been derived as follows:

$$\frac{\partial}{\partial t}\overline{\rho C_{p2}}\Theta_2 + d_3\frac{\partial^{\gamma'}\Theta_2}{\partial t^{\gamma'}} + d_1\frac{\partial^{\beta'}\Theta_2}{\partial t^{\beta'}} = -\frac{\partial \rho_w C_{pw} v \Theta_2}{\partial x}, \tag{6}$$

where $\overline{\rho C_{p2}} = \phi_2\rho_w C_{pw} + (1-\phi_2)\rho_{r2}C_{pr2}$, and ρ_w and ρ_{r2} are the density of water and rock in the main conduit, respectively. C_{pw} and C_{pr2} are the heat capacity of water and rock in the main conduit, and Θ_2 is temperature in the main conduit. The coefficients d_1 and d_3 represent retardation processes caused by the heat diffusivities into the surrounding rocks and into the matrix; $\beta'(0<\beta'\leq 1)$ and $\gamma'(0<\gamma'\leq 1)$ are the orders of fractional derivatives. In Eq. (6), thermal conduction inside the main conduit is negligible, as indicated by Woods and Fitzgerald (1993). In Suzuki et al. (2014), the governing equation given by Eq. (6) was normalized by using the migration time of a heat front. This study aimed at connecting the fADE and the fHTE. Accordingly, a migration time of tracers, t_{tracer}, was used for normalization of Eq. (6). The variables are introduced as follows:

$$\tau = \frac{t}{t_{tracer}}, \quad X = \frac{x}{l}, \quad T = \frac{\Theta_2 - \Theta_{in}}{\Theta_o - \Theta_{in}}, \quad e_1 = \frac{d_1}{\overline{\rho C_{p2}}}t_{tracer}^{1-\beta'},$$
$$e_3 = \frac{d_3}{\overline{\rho C_{p2}}}t_{tracer}^{1-\gamma'}; \tag{7}$$

where Θ_o is the initial temperature of the reservoir, and Θ_{in} is the temperature of injected water. The normalized equation of the fHTE can be written in the following form:

$$\frac{\partial T}{\partial \tau} + e_3\frac{\partial^{\gamma'}T}{\partial \tau^{\gamma'}} + e_1\frac{\partial^{\beta'}T}{\partial \tau^{\beta'}} = -\frac{\phi_2\rho_w C_{pw}}{\overline{\rho C_{p2}}}\frac{\partial T}{\partial X}. \tag{8}$$

3. Model description

The current investigation aims to illustate the applicability of the fADE and the fHTE and evaluating reservoir performance due to cold-water injection in a fault zone. A numerical reservoir simulator, TOUGH2 (Pruess et al., 1999), was used to generate synthetic production data to reveal influence of the structures in fault zones.

Fig. 3 shows a schematic of the numerical simulation model. The numerical properties are summarized in Table 1. A two dimensional model was used to simulate a reservoir that consists

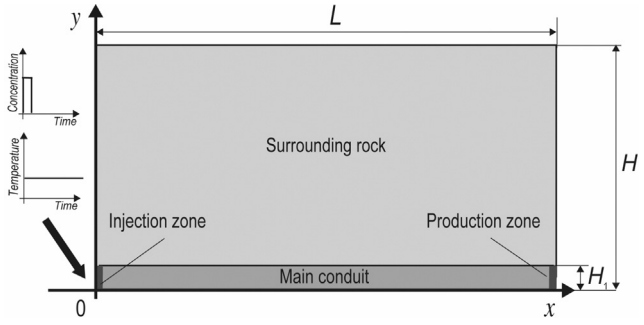

Fig. 3. Schematic of the fault model.

of a main conduit and the surrounding rocks. The impact of gravity was negligible. The thickness H and length L of the calculation domain were set to $H=20$ [m] and $L=100$ [m], respectively. The main conduit was along the fault core, which was parallel to the x-axis. The thickness of the main conduit was set to $H_0=0.2$ [m]. An injection zone and a production zone were located at grids on either side of the main conduit. The grid spacing in the x-axis direction, dx, was 1 m. The grid spacing in the y-axis direction, dy, was more refined closer to the main conduit ($dy=0.2$ [m] in $0\leq y\leq 2.0$, $dy=1.0$ [m] in $2.0\leq y\leq 6.0$, and $dy=2.0$ [m] in $6.0\leq y\leq 20.0$). The discretization was determined to be sufficiently fine because the simulation results had only small differences compared to the result using finer grids.

Table 1
Numerical properties used in TOUGH2.

Property	
Permeability in main conduit	1.0×10^{-13} m^2
Porosity	0.1
Rock density	2600 kg/m^3
Rock heat capacity	1 kJ/kg °C
Thermal conductivity	0 W/m °C
Initial reservoir pressure	10 MPa
Initial reservoir temperature	200 °C
Injection rate	0.2 kg/s
Injection temperature	100 °C
Productivity Index	1×10^{-8} m^3
Production pressure	9 MPa

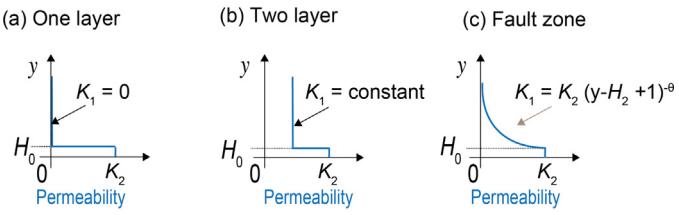

Fig. 4. Permeability distribution for (a) one layer, (b) two layer, and (c) fault zone models.

One-dimensional advective bulk flow traveled from the injection zone towards the production zone. The tracer was continuously injected for 24 h in the injection zone, after which the injection was switched to fresh water. Simulations with the fADE and the fHTE by Eqs. (5) and (8) assumed fluid flow only in the liquid phase. The initial temperature of the reservoir was 200 °C. The temperatures of the tracer and the injected water were 100 °C. The tracer response, i.e., the concentration of tracer, and the temperature histories were observed at the production zone. The productivity index, *PI*, and the production pressure, p_{well}, were determined in a trial-and-error manner. Provided that the rock grains along the fractures are assumed to be sufficiently small and the fluid velocities sufficiently low, local thermodynamic equilibrium between the rock and fluid can be assumed. It was also assumed that the rock is incompressible, that both rock and fluid have constant thermal properties, and that tracer diffusion in the main conduit was negligible. Porosity and rock density were 0.1 and 2500 kg/m^3 for all rocks, respectively.

As noted, fracture density at a damage zone decays with the distance from the fault core according to a power law. In this study, the fracture density is expressed in terms of the permeability, which is taken to be a power law in the following form:

$$K_1(y) = K_2(y - H_0 + 1)^{-\theta}, \tag{9}$$

where K_2 and H_2 are the constant permeability and the thickness of the main conduit, respectively. y is the distance from the main conduit, and θ is the exponent expressing decay of permeability. Note that TOUGH2 solves continuum equations on each grid using an integral finite difference method. Permeability on each grid was determined by the value at the center of the grid.

López and Smith (1995) suggested that advection dominates when permeability at a main conduit is lower than 7×10^{-13} m^2 and permeability in the surrounding rock is higher than 5×10^{-18} m^2. An advection-dominated reservoir is our focus in this study. Thus, the permeability value in the main conduit, K_2, was set to 1.0×10^{-13} m^2, and the permeability value in the surrounding rock, K_1, was set to higher than 1×10^{-16} m^2. In addition, the effect of thermal conductivity was negligible.

The model using the permeability distribution given by Eq. (9) is referred to as the fault zone model. For comparison, two different reservoir models were examined using TOUGH2: a one-layer model and a two-layer model. These models used the same rock parameters as the fault zone model summarized in Table 1. The area surrounding the main conduit in the one-layer model was assumed to be impermeable. The two-layer model has a constant permeability in the surrounding area, K_1, which is lower than K_2. Thus, there is a discontinuous permeability distribution in the y-axis direction. The permeability distribution for each model is illustrated in Fig. 4.

Tracer breakthrough and temperature histories obtained using TOUGH2 were compared with the fADE and the fHTE. The tracer responses and thermal responses calculated using TOUGH2 were normalized using representative physical variables discussed in the previous section. A finite difference approach for discretization used an implicit method in time and an upwind scheme in the advection term was used to solve the fADE and the fHTE (Suzuki et al., 2014).

This study addressed the effect of fault-related structures, which leads to diffusion into the surrounding rocks. Thus, we used constitutive parameters in the third terms on the left-hand side in Eqs. (5) and (8). The effects of diffusion into the matrix, which are described by the second terms on the left-hand side in Eqs. (5) and (8), were negligible. Therefore, the values of b_3 and e_3 were set to 0, and the value of α was set to 1. In addition, this study set the skewness parameter p to 0 because p is known to be less than 0.5 in the case where fluid flow within a reservoir is subject to preferential flow paths, which is consistent with other studies (i.e., Zhang et al., 2007). Hence, the parameters required to fit the tracer and temperature data were b_1, β, and *Pe* in the fADE and e_1 and β' in the fHTE. We determined the parameters by minimizing the root-mean-square error (RMSE) between the simulated data by TOUGH2 and the solutions of the fADE and the fHTE.

4. Results and discussion

Figs. 5(a) and 6(a) show the tracer response and the temperature history obtained from the one-layer model. The tracer response had a symmetric distribution. This is because the tracer transport process was governed solely by advection. The solution of ADE is also plotted in Fig. 5(a). The ADE can capture the tracer response. Fig. 6(a) shows that a rapid thermal breakthrough occurred in the one-layer model.

Tracer responses for the two-layer model are displayed in Fig. 5(b). The permeability in the main conduit was fixed to $K_2 = 1.0 \times 10^{-13}$[m^2], while the permeability in the surrounding rock K_1 was varied over the range of $1.0 - -7.0 \times 10^{-16}$[m^2]. In this case, the tracer responses exhibit long tails and second peaks that depend on the values of K_1. Greater values of K_1 led to heavier tails. Thus, penetration into the surrounding rocks caused the remarkable retardation of the tracers. These double-peak responses are supposed to be the result of two distinct flow pathways between the injection and production zones. The first peak in the tracer response was produced by tracers that migrated directly from the injection zone to the production zone in the main conduit, while the second peak resulted from the other tracers that traveled through the surrounding rocks more or less. Temperature histories for the two-layer model are displayed in Fig. 6(b). Comparing Fig. 6(a) and Fig. 6(b) shows that higher permeability in the surrounding rocks eased the thermal breakthrough.

For the fault zone model, the permeability of the surrounding rocks at the damage zone was defined as in Eq. (9). Fig. 5(c) shows tracer responses for the fault zone model. Compared to the two-layer model (Fig. 5(b)), the fault zone model produced gradual decreases in concentration. It indicates that several flow patterns occurred due to a wide range of permeability of the surrounding rocks in the fault zone model. The superposition of the tracer responses for each flow pattern produced the gradual decreases in concentration. Our results provide a clear distinction in the tracer responses and the temperature between the fault zone model and the two-layer model. They suggest that a model with discontinuous permeability distribution, such as the two-layer model in this study, is insufficient to characterize reservoir performance in a fault zone and that the spatial change in permeability should be considered.

Fig. 7 shows the best-fit curve of the fADE to the calculated tracer response for $\theta = 1.5$ in the fault zone model. For comparison, the best-fit curves of the conventional models are also plotted. The constitutional parameters of each model were determined by minimization of the RMSEs. The ADE is the conventional mass transport model (Bear, 1972). The fitting result shows a more symmetric shape, which is in disagreement with the calculated tracer

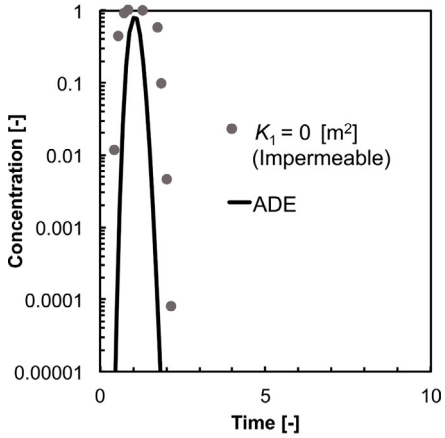

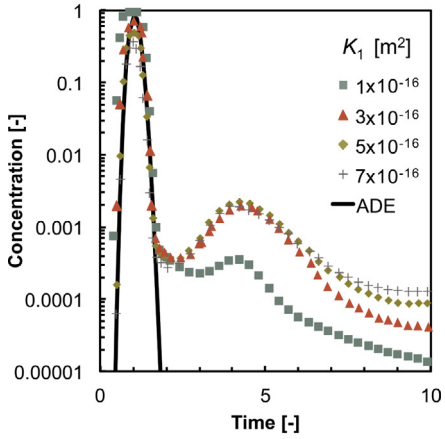

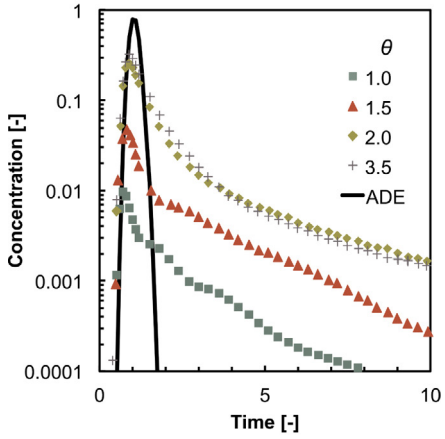

Fig. 5. Effects of permeability distributions on tracer responses calculated by TOUGH2: (a)one layer, (b)two layer, and (c)fault zone models.

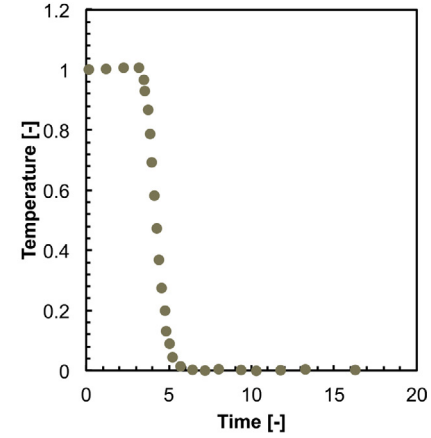

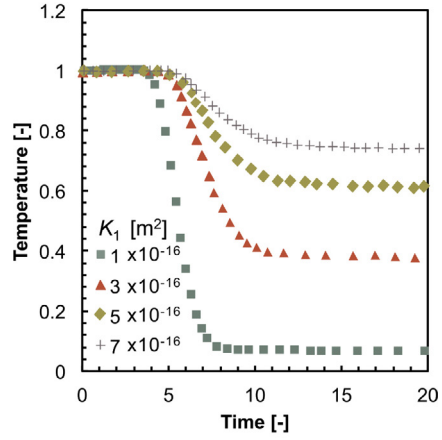

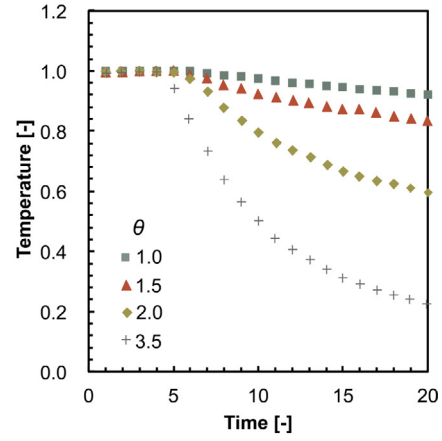

Fig. 6. Effects of permeability distributions on temperature calculated by TOUGH2: (a)one layer, (b)two layer, and (c)fault zone models.

response. The retardation model includes a retardation factor into the ADE (Van Genuchten and Wierenga, 1976). The Fick's diffusion model takes into account the diffusion into the surrounding rock according to the Fick's law. The fitting results of both models were affected by the long-term behavior of tracers but did not match the overall tracer response well. The calculated RMSEs for the ADE, the retardation model, and the Fick's diffusion model were 4.91×10^{-2}, 7.45×10^{-3}, and 6.37×10^{-3}, respectively. On the other hand, as displayed in Fig. 7, the fADE was able to capture the calculated tracer response with an improved fit. The RMSE for the fADE was 2.46×10^{-3}. This result corroborates that the fADE is an appropriate model to describe the tracer response in a fault zone.

Fig. 8 shows the best-fit curves on the calculated temperature for $\theta = 1.5$ for the fault zone model. The parameters of each model were determined by minimization of the RMSEs. Bodvarsson (1972) derived the basic equation for the subsurface temperature field with intergranular flow. Lauwerier (1955) developed an analytical solution for heat transfer in one-dimensional flow with heat loss into confining beds according to the Fick's law. According to Fig. 8, the intergranular flow model cannot describe the temperature decline calculated by TOUGH2, in which the temperature decreased gradually due to penetration into the surrounding rocks. Anomalous diffusion processes are described by the form $<\Delta x> \propto Dt^{\beta}$ (Burnecki et al., 2008). The value of the anomalous diffusion index β distinguishes subdiffusion ($0 < \beta < 0.5$) (slower growth) and superdiffusion ($\beta > 0.5$) (faster growth). The diffusion

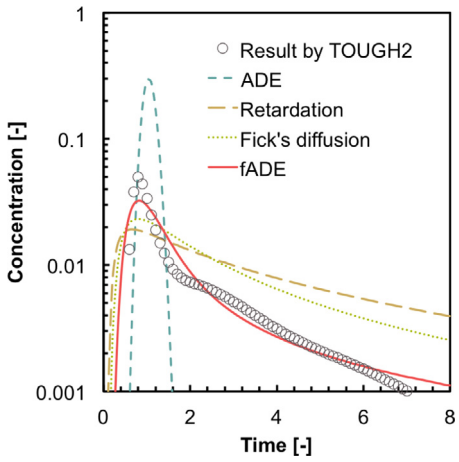

Fig. 7. Simulated tracer response by TOUGH2 using the fault zone model for $\theta = 1.5$ (symbols) and best fits with the conventional models and the fADE (lines).

process for β of 0.5 is considered as Fick's diffusion. Fomin et al. (2011) derived an analytical solution of the fADE and indicated that when the order of fractional derivative β is 0.5, the solution can reduce to the Fick's diffusion model. Therefore, the anomalous diffusion index β is in accordance with the value of β in Eq. (5). As shown in Fig. 8, the fitting result obtained by the Fick's diffusion model was slightly different from the calculated temperature. The result indicates that the thermal diffusion into the surrounding rocks was slower than Fick's diffusion, i.e., subdiffusion occurred. In this simulation, higher permeability in the surrounding rocks led to outflow of the injected water from the main conduit and resulted in the slower decay in temperature at the production zone. In contrast, the fHTE can reproduce the gradual temperature decline curve as illustrated in Fig. 8. The optimized value of β in the fADE was 0.2. The value was consistent with the fact that subdiffusion occurred.

The correlations between θ and the best-fit constitutional parameters in the fADE and the fHTE are plotted in Fig. 9. In the case when θ was less than 1.0, little tracer reached at the production zone during the calculation time (10^{10} s), and tracer response curve was unavailable. In addition, because the permeability for higher values of θ decreases sharply from the main conduit in the surrounding area, the surrounding area is almost impermeable. Then, the tracer responses for θ over 3.5 were much the same. Therefore, the data for θ from 1.0 to 3.5 were used. The recovery rate of tracer at the production zone was smaller for lower values of θ than for greater values of θ. The parameters of the fADE and the fHTE, were

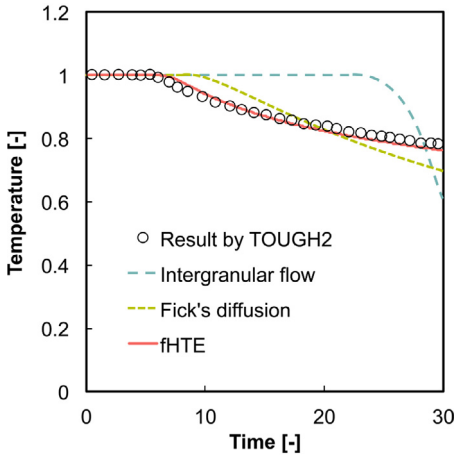

Fig. 8. Simulated temperature by TOUGH2 using the fault model for $\theta = 1.5$ (symbols) and the best fits with the conventional models and the fHTE (lines).

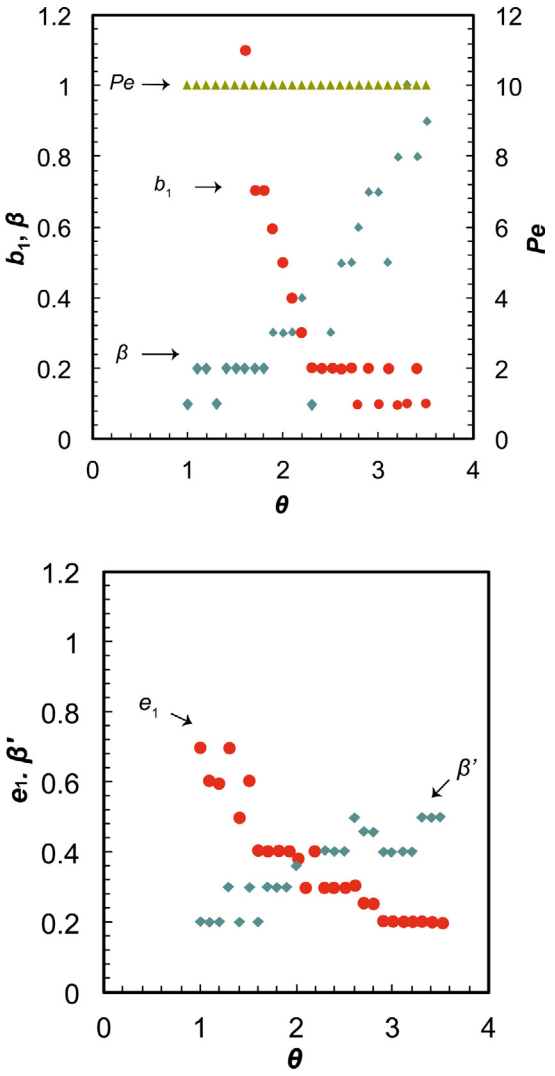

Fig. 9. Relationship between θ and (a) the fADE and (b)the fHTE constitutional parameters.

determined by minimization of the RMSEs. Here, the smaller values of θ caused higher penetration into the surrounding rocks. The smaller values of θ increases the value of the retardation parameters b_1 and e_1 and decreases the orders of the fractional derivatives β and β', respectively. The fADE and fHTE constitutional parameters show the same dependence on θ.

The relationship with θ (excluding Pe) were used for regression analysis. The regression equation for the value of θ is as follow:

$$\theta = 1.53\beta - 0.61b_1 + 2.03. \quad (10)$$

The above equation can be used to estimate θ based on the fADE constitutive parameters. Furthermore, the regression equations to estimate the fHTE constitutional parameters based on the fADE constitutional parameters can be obtained as follows:

$$e_1 = -0.12\beta - 0.17b_1 + 0.25, \quad (11)$$

$$\beta' = 0.15\beta + 0.10b_1 + 0.34. \quad (12)$$

The results of the comparison between the performances of the estimation of θ, e_1, and β are shown in Fig. 10. Each coefficient of determination R^2 was relatively high ($R^2 = 0.975$ for θ, $R^2 = 0.956$ for e_1 and $R^2 = 0.965$ for β).

The regression equations of Eqs. (10)–(12) were verified by using numerical results obtained from TOUGH2. The best-fit fADE

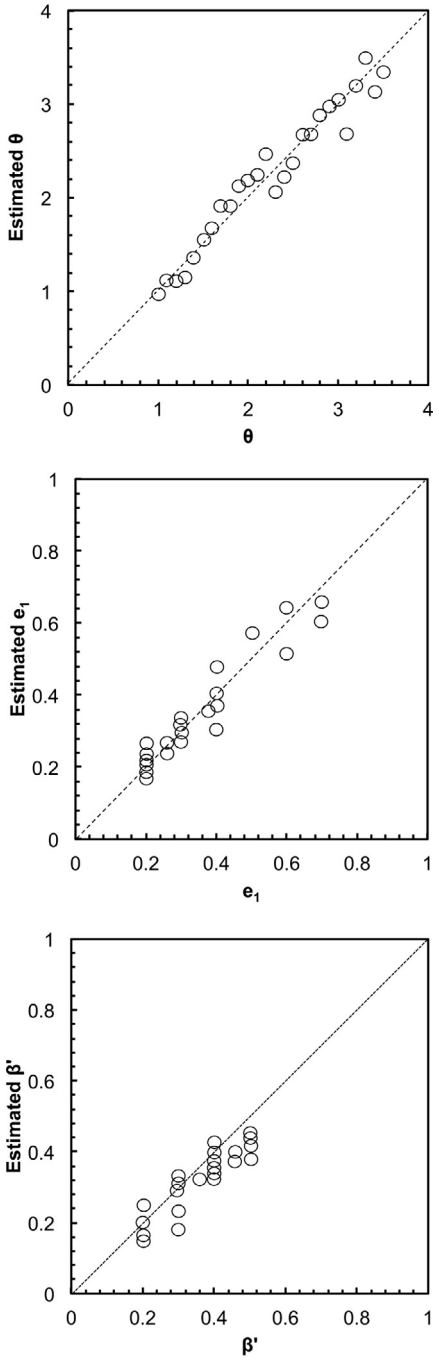

Fig. 10. Estimate accuracy of θ, e_1 and β'; Validity check of the correlation of regression equations.

constitutional parameters for $\theta = 0.1$ were $b_1 = 2.0$, $\beta = 0.1$, and $Pe = 10.0$. Substituting the parameters into Eqs. (10)–(12), θ, e_1 and β were estimated: $\theta = 0.90$, $e_1 = 0.66$, and $\beta = 0.15$. The difference between the actual value and the estimated value was 0.1 for θ. The result suggests the regression equation for θ (Eq. (10)) provides relatively good estimation in this case. Subsequently, the temperature decline simulated by TOUGH2 for $\theta = 1.0$ and the predicted result by using estimated parameters of e_1 and β' were compared. The predicted result of temperature was in good agreement with the simulated result by TOUGH2. The coefficient of determination between actual and estimated temperature change was $R^2 = 0.992$. From the above, the regression equations written in Eqs. (10)–(12) can be applied to estimation of θ, e_1, and β. Thus, the fADE constitutive parameters, which are obtained from tracer data, have potential to provide useful parameters for characterizing the fault-related structure and for predicting temperature history in an advection-dominated reservoir.

Despite significant improvement in computer-aided numerical reservoir simulation, reservoir analysis remains both technically difficult and time-consuming due to the limited amount of information obtained from the small number of boreholes and indirect (e.g., seismic) measurements. This study shows the fADE can summarize the complexity based on fractal geometry and can quickly and efficiently analyze mass transport in a fractured reservoir at an early stage of geothermal development or with limited information obtained from a field. Our result indicates the tracer analysis by the fADE has potential to estimate the parameter θ that can evaluate permeability distributions in a fault zone. Our previous study has demonstrated that the fADE offers a method for predicting tracer responses irrespective of well intervals in a fractured reservoir (Suzuki et al., 2015). The focus of this study was limited to an advection-dominated fault zone where the thermal conductivity was negligible. Future developments from this study will include prediction of thermal breakthrough for different well intervals and optimization of well locations and/or the reinjection conditions. The technique described in this study is expected to be applicable to prediction of occurrence of thermal breakthrough and temperature decline in fractured reservoirs.

5. Conclusions

The fracture density in a geothermal area was well described by a power-law dependence with distance from the fault core. The fractal diffusion coefficient in the fADE can predict a decrease in diffusivity with distance according to a power law and therefore was consistent with the diffusion process in a fault-related structure. A general reservoir simulator, TOUGH2, was used to generate tracer responses and temperature histories resulting from cold-water injection in an advection-dominated reservoir. The results revealed that permeability patterns in the surrounding rocks contribute to the production data. Conventional advection-dispersion models can describe tracer response only for impermeable surrounding rocks. A model with a discontinuous permeability distribution only produced a tracer response including two peaks. In contrast, a permeability distribution of a fault-related structure resulted in a gradual decay in concentration of tracer. The fADE and fHTE solutions were found to be in agreement with the tracer response and the temperature history for the fault zone model simulated in TOUGH2. Regression analysis was conducted to provide regression equations of the fADE constitutive parameters to estimate the geometry of the fault zones and the fHTE constitutional parameters. The tracer analysis method based on the fADE is expected to be powerful tools for developing a reservoir model and predicting premature thermal breakthrough in an advection-dominated reservoir.

Acknowledgements

This work was supported by the Japan Society for the Promotion of Science, under JSPS Postdoctoral Fellowships for Research Abroad (H26-416), whose support is gratefully acknowledged. Comments by two anonymous reviewers, Joseph N. Moore, Roland N. Horne, and Audrey P. Fan greatly helped to improve an earlier version of this article.

References

Adams, E.E., Gelhar, L.W., 1992. Field study of dispersion in a heterogeneous aquifer: 2. Spatial moment analysis. Water Resour. Res. 28 (12), 3293–3307.

Agosta, F., Kirschner, D.L., 2003. Fluid conduits in carbonate? Hosted seismogenic normal faults of central Italy. J. Geophys. Res.: Solid Earth 108 (B4), http://dx.doi.org/10.1029/2002JB002013
Aksoy, N., Serpen, U., Filiz, Ş., 2008. Management of the Balcova-Narlidere geothermal reservoir, Turkey. Geothermics 37 (4), 444–466.
Axelsson, G., 2010. Sustainable geothermal utilization: case histories; definitions; research issues and modelling. Geothermics 39 (4), 283–291.
Baeumer, B., Benson, D.A., Meerschaert, M.M., Wheatcraft, S.W., 2001. Subordinated advection-dispersion equation for contaminant transport. Water Resour. Res. 37 (6), 1543–1550.
Bear, J., 1972. Dynamics of Fluids in Porous Media. Elsevier, New York.
Benson, D.A., Wheatcraft, S.W., Meerschaert, M.M., 2000. Application of a fractional advection-dispersion equation. Water Resour. Res. 36 (6), 1403–1412.
Bodvarsson, G., 1972. Thermal problems in the siting of reinjection wells. Geothermics 1 (2), 63–66.
Bödvarsson, G.S., Tsang, C.F., 1982. Injection and thermal breakthrough in fractured geothermal reservoirs. J. Geophys. Res.: Solid Earth 87 (B2), 1031–1048.
Bonnet, E., Bour, O., Odling, N.E., Davy, P., Main, I., Cowie, P., Berkowitz, B., 2001. Scaling of fracture systems in geological media. Rev. Geophys. 39 (3), 347–383.
Brock, W.G., Engelder, T., 1977. Deformation associated with the movement of the Muddy Mountain overthrust in the Buffington window, southeastern Nevada. Geol. Soc. Am. Bull. 88 (11), 1667–1677.
Brogi, A., 2008. Fault zone architecture and permeability features in siliceous sedimentary rocks: insights from the Rapolano geothermal area (Northern Apennines, Italy). J. Struct. Geol. 30 (2), 237–256.
Burnecki, K., Janczura, J., Magdziarz, M., Weron, A., 2008. Can one see a competition between subdiffusion and Lévy flights? A case of geometric-stable noise. Acta Phys. Pol. B 39 (5), 1043–1054.
Caine, J.S., Evans, J.P., Forster, C.B., 1996. Fault zone architecture and permeability structure. Geology 24 (11), 1025–1028.
Chester, F.M., Logan, J.M., 1986. Implications for mechanical properties of brittle faults from observations of the Punchbowl fault zone, California. Pure Appl. Geophys. 124 (1–2), 79–106.
De Joussineau, G., Aydin, A., 2007. The evolution of the damage zone with fault growth in sandstone and its multiscale characteristics. J. Geophys. Res.: Solid Earth 112 (B12), http://dx.doi.org/10.1029/2006JB004711
Faulkner, D.R., Jackson, C.A.L., Lunn, R.J., Schlische, R.W., Shipton, Z.K., Wibberley, C.A.J., Withjack, M.O., 2010. A review of recent developments concerning the structure, mechanics and fluid flow properties of fault zones. J. Struct. Geol. 32 (11), 1557–1575.
Fomin, S., Chugunov, V., Hashida, T., 2005. The effect of non-Fickian diffusion into surrounding rocks on contaminant transport in a fractured porous aquifer. Proc. R. Soc. A: Math. Phys. Eng. Sci. 461 (2061), 2923–2939.
Fomin, S.A., Chugunov, V.A., Hashida, T., 2011. Non-Fickian mass transport in fractured porous media. Adv. Water Resour. 34 (2), 205–214.
Gringarten, A.C., Sauty, J.P., 1975. A theoretical study of heat extraction from aquifers with uniform regional flow. J. Geophys. Res. 80 (35), 4956–4962.
Gudmundsson, A., 2011. Rock Fractures in Geological Processes. Cambridge University Press.
Kaya, E., Zarrouk, S.J., O'Sullivan, M.J., 2011. Reinjection in geothermal fields: a review of worldwide experience. Renew. Sustain. Energy Rev. 15 (1), 47–68.
Kocabas, I., 2005. Geothermal reservoir characterization via thermal injection backflow and interwell tracer testing. Geothermics 34 (1), 27–46.
Huang, Q., Huang, G., Zhan, H., 2008. A finite element solution for the fractional advection-dispersion equation. Adv. Water Resour. 31 (12), 1578–1589.
Lauwerier, H.A., 1955. The transport of heat in an oil layer caused by the injection of hot fluid. Appl. Sci. Res. Sect. A 5 (2-3), 145–150.
Le Garzic, E., de L'Hamaide, T., Diraison, M., Géraud, Y., Sausse, J., de Urreiztieta, M., Hauville, B., Champanhet, J.M., 2011. Scaling and geometric properties of extensional fracture systems in the proterozoic basement of Yemen. Tectonic interpretation and fluid flow implications. J. Struct. Geol. 33 (4), 519–536.
López, D.L., Smith, L., 1995. Fluid flow in fault zones: analysis of the interplay of convective circulation and topographically driven groundwater flow. Water Resour. Res. 31 (6), 1489–1503.
Massart, B., Paillet, M., Henrion, V., Sausse, J., Dezayes, C., Genter, A., Bisset, A., 2010. Fracture Characterization and Stochastic Modeling of the Granitic Basement in the HDR Soultz Project (France). World Geothermal Congress, pp. 2010.
Pruess, K., Oldenburg, C.M., Moridis, G.J., 1999. TOUGH2 User's Guide, Version 2.0. Lawrence Berkeley National Laboratory, LBNL-43134.
Pruess, K., Bodvarsson, G.S., 1984. Thermal effects of reinjection in geothermal reservoirs with major vertical fractures. J. Petrol. Technol. 36 (10), 1567–1578.
Samko, S.G., Kilbas, A.A., Marichev, O.I., 1993. Fractional Integrals and Derivatives: Theory and Applications. Gordon and Breach, London.
Sanjuan, B., Pinault, J.L., Rose, P., Gérard, A., Brach, M., Braibant, G., Crouzet, C., Foucher, J.C., Gautier, A., Touzelet, S., 2006. Tracer testing of the geothermal heat exchanger at Soultz-sous-Forêts (France) between 2000 and 2005. Geothermics 35, 622–653.
Savage, H.M., Brodsky, E.E., 2011. Collateral damage: Evolution with displacement of fracture distribution and secondary fault strands in fault damage zones. J. Geophys. Res.: Solid Earth 116 (B3), B03405.
Shook, G.M., 2001. Predicting thermal breakthrough in heterogeneous media from tracer tests. Geothermics 30 (6), 573–589.
Shook, G.M., 2003. A simple, fast method of estimating fractured reservoir geometry from tracer tests. Geoth. Resour. Counc. Trans. 27, 407–411.
Schumer, R., Benson, D.A., Meerschaert, M.M., Baeumer, B., 2003. Fractal mobile/immobile transport. Water Resour. Res. 39 (10), http://dx.doi.org/10.1029/2003WR002141
Suzuki, A., Makita, H., Niibori, Y., Fomin, S.A., Chugunov, V.A., Hashida, T., 2014. Analysis of water injection in fractured reservoirs using a fractional-derivative-based mass and heat transfer model. Math. Geosci. 47 (1), 31–49.
Suzuki, A., Niibori, Y., Fomin, S., Chugunov, V., Hashida, T., 2015. Fractional derivative-based tracer analysis method for the characterization of mass transport in fractured geothermal reservoirs. Geothermics 53, 125–132.
Van Genuchten, M.T., Wierenga, P.J., 1976. Mass transfer studies in sorbing porous media I. Analytical solutions. Soil Sci. Soc. Am. J. 40, 473–480.
Welty, J., Wicks, C.E., Rorrer, G.L., Wilson, R.E., 2009. Fundamentals of Momentum, Heat and Mass Transfer. Wiley, New York.
Woods, A.W., Fitzgerald, S.D., 1993. The vaporization of a liquid front moving through a hot porous rock. J. Fluid Mech. 251, 563–579.
Zhang, Y., Benson, D.A., Reeves, D.M., 2009. Time and Space Nonlocalities Time and space nonlocalities underlying fractional-derivative models: Distinction and literature review of field applications. Adv. Water Resour. 32 (4), 561–581.
Zhang, X., Lv, M., Crawford, J.W., Young, I.M., 2007. The impact of boundary on the fractional advection-dispersion equation for solute transport in soil: defining the fractional dispersive flux with the Caputo derivatives. Adv. Water Resour. 30, 1205–1217.